On Femto placement and *decoupled* access for downlink and uplink in enterprise environments

Vanlin Sathya[1,*], Arun Ramamurthy[1], Milind Tahalani[2], Bheemarjuna Reddy Tamma[1]

[1]Department of Computer Science and Engineering, Indian Institute of Technology Hyderabad, India.
[2]Department of Mathematics, Indian Institute of Technology Kharagpur, India.

Abstract

While it is easier to quench the demand for higher data rates outdoors, it is still a significant challenge when it comes to attaining similar data rates for indoor User Equipments (UEs). Femto cells were introduced for this purpose and also to minimize the traffic load on macro Base Stations (BSs) in 4G/LTE cellular networks. Indoor UEs can achieve good throughput if they get high Signal to Noise Ratio (SNR), but the inherent problem of path loss due to obstacles prevents UEs from receiving good signals. So, the efficient placement of Femtos in enterprise buildings is crucial. For the optimal placement of Femtos, we developed a Mixed Integer Linear Programming (MILP) model and solved it using the GAMS tool. Once the network planning is done, the next problem that has to be addressed is the downlink traffic imbalance which happens due to non-uniform UE traffic distribution. Traditionally load imbalance is addressed by transferring some of the UEs from the highly loaded cell to a less loaded neighboring cell but this could increase the UE uplink transmission power as it now connected to a cell which is not the closest one. To improve UE battery life and to boost the downlink throughput, we *decouple* the uplink and downlink (DuD) access to UEs by connecting the uplink to the shortest pathloss Femto, and the downlink to one of less loaded neighboring Femtos. Our extensive experimentation in MATLAB shows that on average, the *decoupled* access system achieves 70% energy savings (i.e., uplink power) when compared to *coupled* access system.

1. Introduction

The generation of smartphones and tablets has seen a tremendous increase in the demand for higher data rates. While 3G data provided by mobile operators serves basic purposes, Long Term Evolution (LTE) is tipped to provide the best data rates for meeting ever increasing demands in outdoor environments. According to a study made by Cisco and Huawei [1], the need to address high traffic in indoor environments is high. Poor coverage and path loss due to obstacles like walls and floors inhibit the existing outdoor Base Stations (BS) providing good indoor coverage in multi-storey buildings. Better data rates could be achieved in indoor for User Equipments (UEs) by deploying more macro BSs, but this would increase Capital Expenditure (CAPEX) and Operational Expenditure (OPEX) incurred by the mobile operator. In order to satisfy the demand of indoor UEs in low CAPEX,

deploying Low Power Nodes (LPNs) a.k.a. Femto BSs [2], is an amenable solution. Femto (a.k.a. Home eNodeB and enterprise eNodeB) is a low power plug-and-play BS designed for covering small regions like homes and offices. Bulk deployment of Femtos in enterprise environments could substantially enhance user experience of cellular systems. Femtos have the capability to serve around 20 to 30 users within the coverage range of at most 60 meters and Femtos get connected to a centralized Femto-GW (refer Fig. 1) using S1 interface for interference and handover management.

The dense deployment of Femtos in enterprise environments [3] necessitates the need for their optimal placement to guarantee good signal strength to all indoor UEs and to minimize coverage holes. Once, the placement of Femtos is done, the other varying parameters that affect the data rate in wireless systems

*Corresponding author. Email: cs11p1003@iith.ac.in

are load and interference. In our work, we concentrate on the former by formulating a Mixed Integer Linear Programming (MILP) model for the optimal placement of Femtos. In a typical indoor scenario with UEs, the uplink load of a cell would more or less be the same in the entire building, but the downlink load of the cell would vary from one Femto to other depending on the number of UEs being served [4, 5], and their traffic demands. In traditional cellular networks, the uplink access and downlink access are *coupled* to the same BS as shown in Fig. 1. The user U_t uses $Femto_2$ for both uplink and downlink communication because the signal strength from $Femto_2$ is very high for the user U_t. Suppose a Femto is fully loaded when compared to its neighboring Femtos, the traditional offloading or load balancing algorithms [6, 7] will shift some of the UEs for both uplink and downlink from the loaded cell to one of less loaded cells (target cells) provided that these UEs still could get connected to the target cell. This type of offloading is a forced handover based on the load but not based on signal strength, because the signal strength when connected to the initial serving Femto will be high compared to the target Femto. For example in Fig. 1, we observe that $Femto_2$ is heavily loaded so the user u_t can be offloaded to the neighboring Femto i.e., $Femto_1$. In a *coupled* access system, as shown in Fig. 2, after offloading u_t uses $Femto_1$ for both uplink and downlink communication. Since u_t and $Femto_1$ are separated by a wall, u_t has to transmit with a higher power in $Femto_1$ compared to $Femto_2$. By doing this offloading approach, the overall system throughput will boost but the uplink power of the shifted UEs would increase and there by drain their batteries.
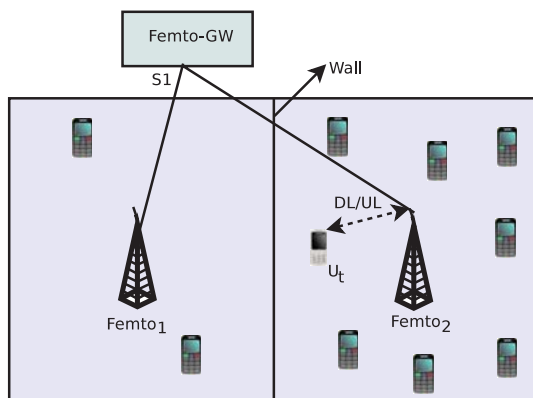

Figure 1. *Coupled* Access System before offloading U_t to $Femto_1$.

In order to reduce the battery drain from UEs and to boost the downlink data rate, one could use the *Decoupled* uplink and downlink (DuD) access method i.e., uplink connected to the closest Femto and downlink to a less loaded Femto. In this work,
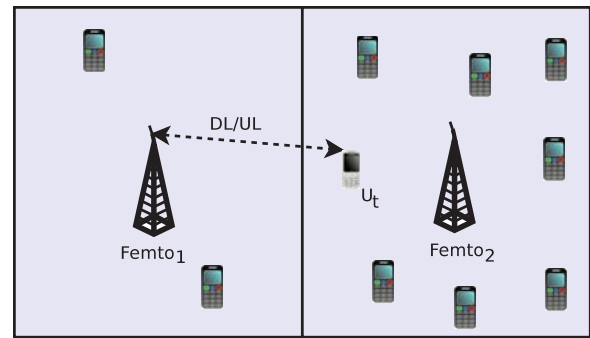

Figure 2. *Coupled* Access System after offloading U_t to $Femto_1$ from $Femto_2$.
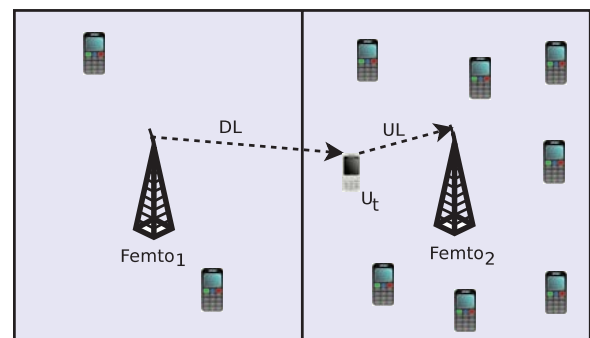

Figure 3. *Decoupled* Access System after offloading only donwlink of U_t to $Femto_1$ from $Femto_2$.

the Femto which is closest (highest SNR) to an UE is called as *serving* Femto and the neighboring/target Femtos are called as *target* Femtos. For example in Fig. 3, we observe that user u_t uses $Femto_1$ for downlink and $Femto_2$ for uplink communication which saves its UE battery. Before doing this, the placement of Femtos should be optimal inside the building to attain a desirable SNR (Signal-to-Noise Ratio) for indoor UEs.

In the present work, we placed Femtos optimally to obtain a desirable SNR. Two major parameters that determine the optimal Femto locations include (i) distance between Femto and the farthest point inside the building and (ii) the minimum SNR needed by each UE. Solving for optimal placement of Femtos by considering the above parameters results in a non-convex optimization problem. We further simplify this non-convex problem to fit into MILP model and solve it using GAMS tool [8]. To increase the downlink throughput and reduce battery drain, we propose an offloading algorithm in DuD access system.

The rest of the paper is organized as follows. Section 2 presents related work on Femto placement and *decouped* access systems. Section 3 describes the proposed work in Femto placement. Section 4 presents the proposed efficient offloading algorithm for *decouped*

access systems. In Section 5, we show the performance results of the proposed Femto placement model and offloading algorithm in a two-storey enterprise building scenario. Finally, Section 6 presents conclusions and directions for future work.

2. Related Work

In order to boost the data rate, Femtos were introduced by 3GPP. Right from its incorporation, extensive research has been carried out to improve Femto placement architectures considering various issues like frequent hand-offs, interference and physical cell ID (PCID) [3]. An effective algorithm for the optimal placement of Femtos depends on the distance between the first Femto and the macro BS, as given in [9, 10], but the work does not consider the Femto to Femto interference inside the building. Works on optimal relay node placement in tunnels [11], sensor placement [12, 13] in terrain regions and optimal placement of Wi-Fi APs [14] exist in literature. In [15], we studied placement of the Femtos optimally inside a building while securing good SINR for UEs by considering cross-tier and co-tier interference between Macro BSs and the Femtos. In [16], we studied joint Femto placement and power control for guaranteeing SINR threshold depending on user occupancy in each region inside the building. However, MILP models proposed in our previous works [15, 16] target to ensure SINR threshold only at the center of the sub-regions (*i.e.,* sub-region is of length δ_x and width δ_y, explained in detail latter) inside the building and hence they fail to guarantee at all the farthest points of the sub-regions. In this work, we have not considered inter-Femto interference (*i.e.,* co-tier interference) and Macro-BS interference (*i.e.,* cross-tier interference) in the system model. But our optimization model guarantees good SNR at the farthest points in the sub-regions inside the building. The algorithm for optimal Femto placement provided in [17, 18] is of limited practical value since it ignores walls inside the buildings while determining Femto locations. Appending to the above work, we constrained the problem to be similar to realistic enterprise buildings by considering the path loss across walls inside the building. The resulting non-convex optimization model is solved by approximating it as an MILP.

After placing the Femtos optimally to guarantee good signal strength at the farthest points inside the sub-region of the building, the other problem that arises is load-imbalance across Femtos. Lot of existing literature discuss about the load balancing in LTE systems by varying the handover hysteresis margin, dynamic BS power control [15] and centralized load balance using software defined network (SDN)

approaches. In [6, 7, 19] authors proposed a multi-objective problem with the objective of load balance by meeting QoS requirements and the network utility of other services like voice, video and online gaming, but the running time complexity of the proposed optimization problem is high. So, they proposed a practical algorithm which considers QoS guaranteed hybrid scheduling, handover of users with and without QoS requirements and call admission control. In [20], we designed a self organizing network (SON) triggered load balance/handover algorithm which takes into account the building layout to avoid ping-pong effect.

All these traditional load balancing techniques increase the battery power consumption of the UE who is being offloaded from heavily loaded Femto to lightly loaded Femto since the distance for the uplink access is high in *coupled* access systems. In order to save energy, *decoupling* is the efficient solution without degrading the performance of the UE. Along these lines, in the first work [21, 22], authors proposed a way in which the uplink connects to one of less path loss small cells and the downlink connects to a macro BS, causing a reduction in the uplink power, but also decreases the downlink throughput due to path losses encountered in reaching the UE indoors.

In [23], we focused on the optimal placement of Femtos inside the building using a MILP model. In this work, we extend the work done in [23] by proposing an efficient offloading algorithm in DuD access system for addressing load imbalance in Femto cells.

3. Optimal Femto Placement

In this section, we present Femto placement in enterprise building environments as an optimization problem.
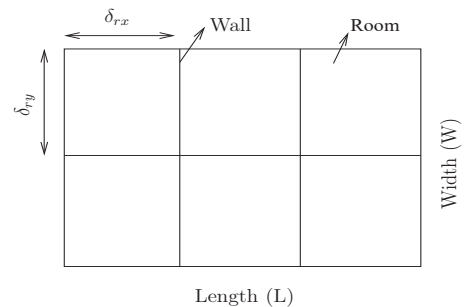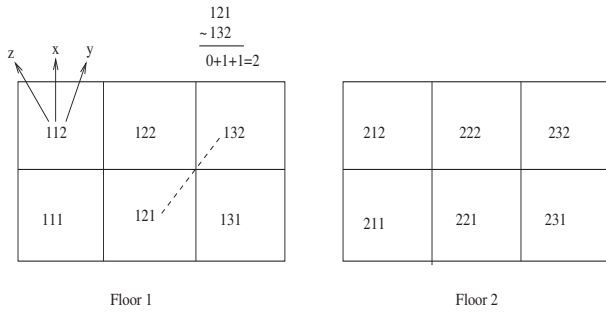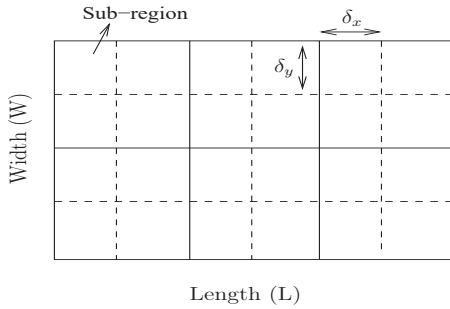
3.1. Building Model

Figure 4. Top view of a floor in the building.

The enterprise building is considered to be of length L and width W. Let, the height of each floor be h. Each floor is further partitioned into rooms of equal dimensions as illustrated in Fig. 4. The length and

EAI
European Alliance
for Innovation

3

EAI Endorsed Transactions on
Future Internet
03 – 05 2016 | Volume 3 | Issue 9 | e2

Figure 5. Numbering of rooms and calculation of number of walls between Femto and sub-region.

Figure 7. Numbering of sub-regions on floor #1 and floor #2.

width of each room are δ_{rx} and δ_{ry}, respectively. Each room is numbered ρ_{zxy}, also be denoted as $\rho_z\rho_x\rho_y$. The first digit in three digit numerical scheme signifies the floor number, second digit varies along X- axis and the third digit varies along Y-axis as shown in Fig. 5. If the room number is referred to as ρ_x, it implies that the room number is varied along the X-axis only. For e.g. if $\rho_{zxy} = 122$ and if $\rho_x + 1$ operation is applied, then $\rho_{zxy} = 132$.
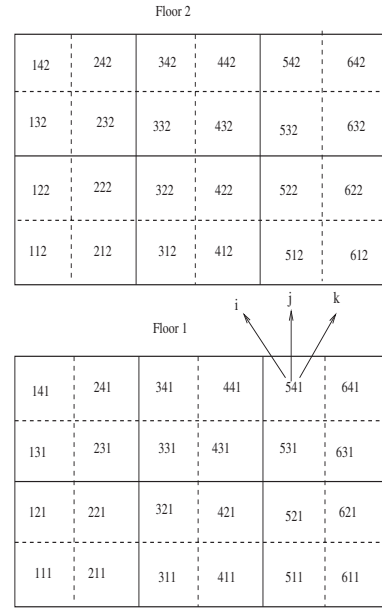

Figure 6. Top view of sub-regions in the building.

We assume that F Femtos are available to cover the entire building and they are to be placed only on the ceiling of the rooms. ρ_f denotes the room number of fth Femto. We further divide each room into sub-regions as shown in Fig. 6. The sub-regions are formed for ease of calculations. The length and width of each sub-region are δ_x and δ_y, respectively. The sub-regions are numbered with indices (i, j, k). The first index in the adopted triplet scheme (i, j, k), varies along the X- axis, the second index varies along the Y- axis and the third index designates the floor number as shown in Fig. 7.

3.2. System Model

In this work, we consider an LTE system where Femtos are deployed by network providers, each operating in a different frequency, i.e., no co-tier interference. Also the cross-tier interference between macro BS and

Femtos is ignored. We assume that the existing joint resource allocation [24, 25] algorithms can be applied for avoiding co-tier and cross-tier interference. We also assume that Femtos are configured in open access where UEs are authorized to connect with any of the Femtos. All Femtos deployed in an enterprise building get connected to the centralized Femto-GW. In this work we assume the height h of all floors is same, and the length L and width W of all rooms are same. Additionally, the length δ_x and width δ_y of each sub-region is constant and h_m is the average height of an UE.

The proposed offloading algorithm in DuD access system will be running in a centralized Femto-GW to address the offloading in Femto cells. The SON feature in Femto-GW can automate the offloading algorithm efficiently.

3.3. Formulation of Femto Placement Model

Let us suppose that a given Femto f has the co-ordinates x_f, y_f and z_f. Then, the distance from the Femto to the farthest point in a sub-region defined by (i, j, k) is given by d_{ijk}^f (from reference [18], Fig. 2). Table 1 shows the notation used in MILP formulation.

$$(d_{ijk}^f)^2 = (|x_f - (i - \frac{1}{2})\delta_x| + \frac{1}{2}\delta_x)^2$$
$$+ (|y_f - (j - \frac{1}{2})\delta_y| + \frac{1}{2}\delta_y)^2 + ((z_f - k + 1)h - h_m)^2 \quad (1)$$

We define a binary variable $\lambda_{f\rho}$ as 1 if the fth Femto is in room ρ, and 0 otherwise. z_f co-ordinate of a Femto is

Table 1. Glossary of MILP Model

Notation	Definition
d_{ijk}^f	Farthest distance between Femto f and sub-region (i,j,k).
F	Set of Femtos
x_f, y_f, z_f	x, y and z are the co-ordinates of Femto f.
π_{ijk}^f	1 if Femto f is places at sub-region (i, j, k), zero otherwise.
ρ^f	Represents the room number of Femto f.
ρ_{ijk}	Represents the room number of sub-region i, j, k.
N	Total number of rooms in the building.

an integer indicating the Femto's residing floor number is shown by,

$$z_f = \sum_{\rho=1}^{N} \rho_z \lambda_{f\rho} \tag{2}$$

where N is the number of rooms in the building. Let us assume that f^{th} Femto is residing in the room number ρ_{zxy}. The x and y co-ordinates of the Femto are constrained to be within the bounds of the room in which it is contained as shown in Fig. 8.

Equations (3) and (4) give that the x co-ordinate of the Femto should have the value greater than the left wall and less than the right wall, respectively further represented in Fig. 8.
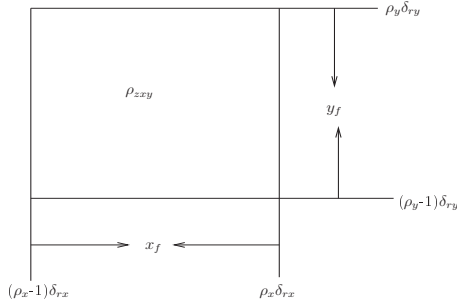
Figure 8. Upper and lower bounds for x_f and y_f

$$x_f \geq \sum_{\rho_x=1}^{N} (\rho_x - 1)\delta_{rx}\lambda_{f\rho} \tag{3}$$

$$x_f \leq \sum_{\rho_x=1}^{N} \rho_x \delta_{rx}\lambda_{f\rho} \tag{4}$$

Similarly, Equations (5) and (6) give that the y co-ordinate of the Femto should have the value greater than the lower wall and less than upper wall, respectively.

$$y_f \geq \sum_{\rho_y=1}^{N} (\rho_y - 1)\delta_{ry}\lambda_{f\rho} \tag{5}$$

$$y_f \leq \sum_{\rho_y=1}^{N} \rho_y \delta_{ry}\lambda_{f\rho} \tag{6}$$

Assuming that a sub-region is served by only one Femto, we have,

$$\sum_{f=1}^{F} \pi_{ijk}^f = 1 \tag{7}$$

The efficiency of a Femto in serving the UEs in a sub-region depends on the SNR value in that sub-region. We set a constraint that the SNR value at the farthest point of the sub-region should be higher than the threshold SNR, γ_{min}. This would imply that every point in the sub-region would receive SNR greater than γ_{min}, since SNR decreases with increasing distance from the Femto. The SNR inside the sub-region (i,j,k), γ_{ijk} is given by

$$\gamma_{ijk} = \frac{P_f}{L_{r_{ref}} \left(\frac{d_{ijk}}{r_{ref}}\right)^{\alpha} P_N} \tag{8}$$

Here P_f is the Femto's transmit power, P_N is the noise power, d_{ijk} is the distance between the sub-region (i, j, k) and the serving Femto, $L_{r_{ref}}$ is the loss at the reference distance r_{ref} in linear scale and α is the path-loss exponent. SNR in dB scale is given by,

$$\gamma_{ijk}^* = P_f^* - L_{r_{ref}}^* - 10\alpha \log_{10}\left(\frac{d_{ijk}}{r_{ref}}\right) - P_N^*$$

where, γ_{ijk}^*, P_F^*, P_N^*, $L_{r_{ref}}^*$ are in dB scale. Considering the attenuation factors for the SNR, the total attenuation is given by,

$$L_{TAF}^* = L_{FAF}^* + L_{WAF}^* \tag{9}$$

where, L_{TAF}^* is total attenuation factor and L_{FAF}^* and L_{WAF}^* are the losses due to floor attenuation and wall attenuation respectively. SNR in dB scale considering wall and floor losses is given by,

$$\gamma_{ijk}^* = P_F^* - L_{r_{ref}}^* - 10\alpha \log_{10}\left(\frac{d_{ijk}}{r_{ref}}\right) - P_N^* - L_{TAF}^* \tag{10}$$

We assume two more variables for the reciprocal of SNR values. Let,

$$\gamma'_{ijk} = \frac{1}{\gamma_{ijk}} \quad (11)$$

γ_{min} is the threshold value of SNR and its reciprocal is γ'_{min}.

$$\gamma'_{min} = \frac{1}{\gamma_{min}} \quad (12)$$

Now Equation (8) can be rewritten as [18]:

$$(d_{ijk})^{\alpha} G(\rho)\Delta^{\rho_f \sim \rho_{ijk}} - \gamma'_{ijk} = 0 \quad (13)$$

$F(\rho)$ is a function defined by,

$$G(\rho) = \begin{cases} K_0 = \frac{C_0 P_n L_{r_{ref}}}{P_f r_{ref}^{\alpha}}, & \text{if } \rho_f \neq \rho_{ijk} \\ K_1 = \frac{C_1 P_n L_{r_{ref}}}{P_f r_{ref}^{\alpha}}, & \text{if } \rho_f = \rho_{ijk} \end{cases} \quad (14)$$

Here C_0 and C_1 are constants depending on the environment. Δ is also a constant depending on the environment and $\rho_f \sim \rho_{ijk}$ is calculated in such a way that it gives the number of obstructions (walls or floors) between the sub-region (i, j, k) and the fth Femto. This special difference ($\sim$) is the absolute value of the digit wise difference between ρ_f and ρ_{ijk} as shown in Fig. 5. For e.g.

a) consider $\rho_f = 121$ and $\rho_{ijk} = 132$.
$\rho_f \sim \rho_{ijk} = 121 \sim 132 = |1 - 1|\beta_1 + (|2 - 3| + |1 - 2|)\beta_2 = 2\beta_2$. Here, $\beta_1 = T_{FAF}$, $\beta_2 = T_{WAF}$. Hence, the rooms 121 and 132 are separated by two walls.

b) consider $\rho_f = 121$ and $\rho_{ijk} = 231$.
$\rho_f \sim \rho_{ijk} = 121 \sim 231 = |1 - 2|\beta_1 + (|2 - 3| + |1 - 1|)\beta_2 = \beta_1 + \beta_2$. The Co-efficient of β indicates the number of floors separating the fth Femto and the sub-region (i, j, k). The co-efficient of β_2 indicates the number of walls separates f^{th} Femto and sub-region (i, j, k). So, the rooms 121 and 231 are separated by one floor and one wall.

Since the SNR received in any sub-region should be greater than the threshold SNR, we have,

$$\gamma'_{ijk} \leq \gamma'_{min} \quad (15)$$

The above constraint (Equation (15)) is ensured for all the sub-regions whose occupant probability is greater than zero (i.e., $p_{ijk} > 0$). If p_{ijk} is the expected peak user density in sub-region (i, j, k), then the placement of Femtos should be in such a way that the product, $p_{ijk}\gamma_{ijk}$ should be maximum for all the sub-regions. Alternately, the product $p_{ijk}\gamma'_{ijk}$ should be minimum. Hence, our objective is

$$min \sum_{ijk} p_{ijk}\gamma'_{ijk}$$

subject to (1), (2), (3), (4), (5), (6), (7), (13) and (15).

But Equations (1) and (13) are non-convex equations which cannot be solved by the available tools. Hence, these equations are first converted to convex equations and then to linear equations.

Linearization of Equation (1):

Let,

$$R^f_{ijk} = (d^f_{ijk})^2 \quad (16)$$

$$X_{fi} = |x_f - (i - \tfrac{1}{2}\delta_x)| \quad (17)$$

$$Y_{fj} = |y_f - (j - \tfrac{1}{2}\delta_y)| \quad (18)$$

Without loss of generality, we can convert the equality in the equations into inequalities with the help of Lemma 1 [18] as follows,

Lemma 1. The constraints in Equation (1) can be equivalently replaced by,

$$\left(X_{fi} + \tfrac{1}{2}\delta_x\right)^2 + \left(Y_{fj} + \tfrac{1}{2}\delta_y\right)^2$$
$$+ (hz_f - ((k - 1)h + h_m))^2 - R^f_{ijk} \leq 0 \quad (19)$$

Moreover, the inequality in Equation (19) holds as equality to an optimal solution.

Equations (17) and (18) are expanded as,

$$x_f - X_{fi} \leq (i - \tfrac{1}{2})\delta_x \quad (20)$$

$$x_f + X_{fi} \geq (i - \tfrac{1}{2})\delta_x \quad (21)$$

$$y_f - Y_{fj} \leq (j - \tfrac{1}{2})\delta_y \quad (22)$$

$$y_f + Y_{fj} \geq (j - \tfrac{1}{2})\delta_y \quad (23)$$

Let,

$$X_{fi}^2 = B_{fi}$$

$$Y_{fj}^2 = D_{fj}$$

$$z_f^2 = E_f$$

The above equations can be written as, (with the help of Lemma 1)

$$X_{fi}^2 - B_{fi} \leq 0 \quad (24)$$

$$Y_{fj}^2 - D_{fj} \leq 0 \quad (25)$$

$$z_f{}^2 - E_f \le 0 \qquad (26)$$

Accordingly, Equation (19) becomes,

$$B_{fi} + D_{fj} + h^2 E_f + \delta_x X_{fi} + \delta_y Y_{fj} - 2h((k-1)h + h_m)z_f$$
$$- R_{ijk}^f \le -\frac{1}{4}\delta_x^2 - \frac{1}{4}\delta_y^2 - ((k-1)h + h_m)^2 \quad (27)$$

Using Piece-wise Linear Approximation (PLAP), the convex constraints (24), (25) and (26) are transformed into linear constraints, which steers the deduction of the following equations,

$$\sum_{S=1}^{S_X} w_1^X (X_S)^2 \le B, \ \sum_{S=1}^{S_X} w_1^X (X_S) = X, \ \sum_{S=1}^{S_X} w_1^X = 1 \quad (28)$$

$$\sum_{S=1}^{S_Y} w_2^Y (Y_S)^2 \le D, \ \sum_{S=1}^{S_Y} w_2^Y (Y_S) = Y, \ \sum_{S=1}^{S_Y} w_2^Y = 1 \quad (29)$$

$$\sum_{S=1}^{S_Z} w_3^Z (Z_S)^2 \le E, \ \sum_{S=1}^{S_Z} w_3^Z (Z_S) = z, \ \sum_{S=1}^{S_Z} w_3^Z = 1 \quad (30)$$

where, w_1^X, w_2^Y and w_3^Z are the positive weights between 0 and 1. The X_S, Y_S and Z_S are the S pieces in their respective domains.

Linearization of Equation (13):

Let,

$$v_{ijk}^f = (R_{ijk}^f)^{\frac{\alpha}{2}} \qquad (31)$$

The above equation can be written (with the help of Lemma 1 [18]) as,

$$v_{ijk}^f \ge (R_{ijk}^f)^{\frac{\alpha}{2}} \qquad (32)$$

Let,

$$g_{ijk}^{f\rho} = v_{ijk}^f \lambda_{f\rho} \qquad (33)$$

Then Equation (13) can be written as

$$K_1 \sum_{\rho, \rho \ne \rho_f}^{N} ((\Delta^{\rho \sim \rho_f}) g_{ijk}^{f\rho}) + K_0 g_{ijk}^{f\rho}$$
$$- (1 - \pi_{ijk}^f)\Gamma_{ijk}^f - \gamma_{ijk}' \le 0 \quad (34)$$

Here, Γ_{ijk}^f is the upper bound of $(d_{ijk})^\alpha F(\rho)\Delta^{\rho_f \sim \rho_{ijk}}$. $\bar{v}_{ijk}^f$ is the upper bound for v_{ijk}^f. The Bilinear equation (33) holds good within the bound $0 \le v_{ijk}^f \le \bar{v}_{ijk}^f$ if and only if (from reference [18])

$$g_{ijk}^{f\rho} \ge 0 \qquad (35)$$

$$g_{ijk}^{f\rho} - \bar{v}_{ijk}^f \le 0 \qquad (36)$$

$$\sum_{\rho}^{N} g_{ijk}^{f\rho} - v_{ijk}^f = 0 \qquad (37)$$

We linearize the convex constraint given in Equation (32) by PLAP and then obtain

$$\sum_{S=1}^{S_R} w_s (R_S)^{\frac{\alpha}{2}} - v \le 0, \ \sum_{S=1}^{S_R} w_s (R_S) = R, \ \sum_{S=1}^{S_R} w_s = 1 \quad (38)$$

where, w_s are the positive weights between 0 and 1. R_S are S pieces in their respective domains.

MILP Model

The optimal Femto placement model can be stated as,

$$min \ \sum_{ijk} p_{ijk} \gamma_{ijk}'$$

Subject to
a) Femto placement constraints:
Equations (2), (3), (4), (5), (6), (7), (15)
b) Linear equations equivalent to (1) :
Equations (20), (21), (22), (23), (27), (28), (29), (30)
c) Linear equations equivalent to (13) :
Equations (34), (35), (36), (37), (38)

4. *Decoupled* Uplink and Downlink (DuD) Access for efficient Offloading in Femtocell Networks

For uniform UE distribution, optimal Femto placement model presented in the previous section ensures that there is no coverage hole inside the building. However, the next challenge after deploying the Femtos inside the building is load balancing. In reality, all the Femtos will not be fully loaded all the times. In order to offload, some UEs which are in the cell edge region are offloaded from the heavily loaded *serving* Femto to one of less loaded neighboring (*target*) Femtos. In traditional *coupled* access systems, the uplink power of offloaded UEs increases because the *target* Femto is far from the UE than the *serving* Femto. But DuD access helps the offloaded UE to get the downlink access from the *target* Femto while the uplink access is still from the same *serving* Femto, thereby decreasing the battery depletion at UE.

4.1. Downlink Offloading Algorithm

The algorithm runs at the Femto-GW every *n* Transmission Time Interval (TTIs). We assume that the channel gain remains static for the next *n* TTIs. Using
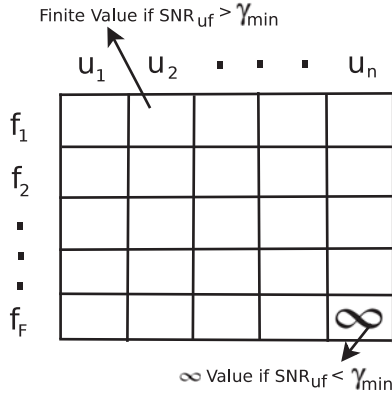
Figure 9. RB Matrix.

the channel gain, the Femto-GW can calculate SNR value of a UE from each Femto. We use SNR_{uf} to denote the SNR value of user u from Femto f. Using SNR_{uf} Femto-GW can calculate the amount of data [26] that can be sent in one resource block (RB). Based on this information, the minimum number of RBs required to maintain the minimum data rate can be calculated. Let $minRB_{uf}$ be the minimum number of RBs required from Femto f to maintain the minimum data rate for user u. Then,

$$minRB_{uf} = \frac{Data\ rate\ Demand_u}{Data\ sent\ in\ one\ RB} \quad (39)$$

Where, $Data\ rate\ Demand_u$ is the minimum data rate of user u and $Data\ sent\ in\ one\ RB$ can be calculated using SNR_{uf}. An RB matrix can be constructed using $minRB_{uf}$ value as shown in Fig. 9.

Before starting the offload algorithm, initially every UE is attached to the *serving* Femto. $TotDemand_f$ is the total demand in Femto f and it can be calculated as,

$$TotDemand_f = \sum_{u \in u_f} minRB_{uf} \quad (40)$$

Where, u_f is the set of UEs connected to Femto f. $minRB$ matrix is constructed using the $minRB_{uf}$ values. A cell is heavily loaded if the $TotDemand$ of the cell is more than $\bar{R}$. Where, $\bar{R}$ is the total available RBs in each Femto. We also define another variable, TED, which is used to calculate the total excess demand in the system.

$$TED = \sum_{f=1}^{F} max(TotDemand_f - \bar{R}, 0) \quad (41)$$

The Femtos are arranged in decreasing order based on their $TotDemand_f$ values. If $TotDemand_f$ is more than $\bar{R}$ for a Femto f then the Femto is picked for offloading. From the $minRB$ matrix find (u^*, f^*) such that $u^* \in$

$u_f, f^* \in F - \{f\}$ and $minRB_{u^*f^*}$ is minimum. Now check if the total RB demand of Femto f^* exceeds $\bar{R}$ if user u^* is offloaded to f^*. If it does not exceed $\bar{R}$, then transfer the UE u^* to Femto f^* and update $TotDemand_{f^*}$ and $TotDemand_f$. If it exceeds $\bar{R}$, then assign a large value to $minRB_{u^*f^*}$ so that the (UE, Femto) pair is not chosen again. Now choose the next best (u^*, f^*) pair and proceed. After transferring a UE if the updated $TotDemand_f$ is less than $\bar{R}$, select the next Femto. After traversing across all the Femtos, calculate the TED value. Stop the algorithm 1 if TED = 0 i.e., every Femto has sufficient RBs to satisfy the user demand. If TED $\neq$ 0, go to step one to repeat Algorithm 1. Stop Algorithm 1 if the TED value remains the same for two iterations.

Algorithm 1 Offloading Algorithm

Input 1 : *F: Set of all Femtos*
Input 2 : *$\bar{R}$: Total available resources in each Femto*
Input 3 : *u_f: Set of all UEs connected to Femto f*
Input 4 : *SNR matrix, minRB matrix*
Input 5 : *$TotDemand_f$: Total RB demand in each Femto*
Input 6 : *TED^0: Initial total excess demand*
Output: u_f

Initialization:
Iteration Count $\leftarrow$ 1;
1: Arrange the Femtos in decreasing order of $TotDemand$ values
2: **for** $f = 1 : |F|$ **do**
3:    **while** $TotDemand_f > \bar{R}$ **do**
4:       Using $minRB$ matrix find a pair (u^*, f^*) such that $u^* \in u_f$, $f^* \in F - \{f\}$ and $minRB$ is the minimum
5:       **if** $(TotDemand_{f^*} + minRB_{u^*f^*}) \leq \bar{R}$ **then**
6:         $TotDemand_{f^*} = TotDemand_{f^*} + minRB_{u^*f^*}$
7:         $TotDemand_f = TotDemand_f - minRB_{u^*f}$
8:         $u_f = u_f - \{u^*\}$
9:         $u_{f^*} = u_{f^*} \cup \{u^*\}$
10:       **else**
11:         $minRB_{u^*f^*}$=Large value {Avoid u^*f^* pair getting selected again}
12:       **end if**
13:       **if** $TotDemand_f \leq \bar{R}$ **then**
14:         Continue (Goto Step 2).
15:       **end if**
16:    **end while**
17: **end for**
18: Update TED^{Count} (using Eqn (41)).
19: **if** $(TED^{Count} == TED^{Count-1}\ or\ TED^{Count} == 0)$ **then**
20:    Exit
21: **else**
22:    Count $\leftarrow$ Count + 1;
23:    Goto Step 1
24: **end if**

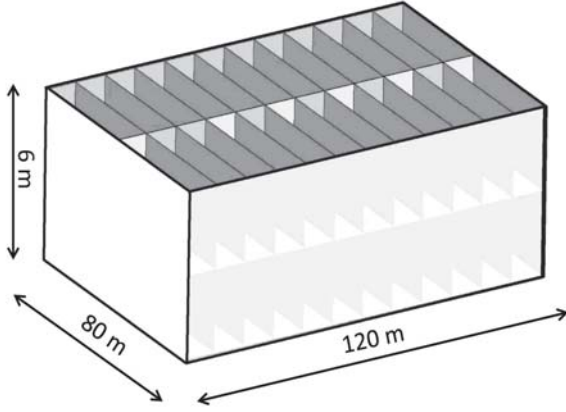**Figure 10.** Two–storey Building

Table 2. Simulation Parameters

Parameter	Value
Building dimensions	120 m × 80 m × 6m
Sub-region dimensions	5 m × 5m × 3m
Number of Sub-regions	384
Number of floors in building	Two
Number of rooms	48
Femto Power	20 dbm
Downlink SNR threshold (γ_{min})	-2 dB
UEs distribution for placement	Uniform
LTE mode	FDD
Femto Bandwidth	5MHz (25 RB)
Simulation time	100 s

4.2. Time complexity of the offloading algorithm

The time complexity of the proposed offloading algorithm is as follows:
Time taken to compute $minRB$ matrix is $O(N * |F|)$, where, N → Total number of users. Number of users who have to be compared for offloading is $O(N)$ and the number of comparisons (with neighboring Femtos) that have to be made for each user is $O(|F|)$. Hence, the total time complexity of the offloading algorithm is $O(N * |F|)$.

5. Experimental Setup and Performance Results

The system model described in Section 3 has been simulated using MATLAB. Table 2 shows the simulation parameters used in this experimental setup. The optimal Femto co-ordinates are obtained by solving MILP model with GAMS tool which uses CPLEX solver [8]. The MILP algorithm is an application of a *branch-and-bound* search including modern algorithmic features such as cuts and heuristics. The MILP optimizer has the capability to solve large and numerically difficult MILP models with features including settable priorities on integer variables, choice of different branching, and node selection strategies. Thus the MILP solver in GAMS (CPLEX) is ideal for our purpose of solving a large MILP model with many equations and variables.

5.1. Optimal Femto Placement

To represent an enterprise scenario, we have considered a two-storey building of dimensions (120m × 80m × 6m) with walls as shown in Fig. 10. Each of its sub-regions are of dimensions (5m × 5m × 3m). We present

placement results for both uniform and non-uniform UE distributions inside the building. As UE density is factored into the proposed optimal Femto placement model, non-uniform UE distribution case could lead to cover holes inside the building.

A. Uniform UE Distribution

For this case, the average user density on the floor #1 of the building is 1.2 UEs per sub-region and on the floor #2 is 1.9 UEs per sub-region. Proposed MILP placement model has given 20 Femtos as optimal to cover both the floors *i.e.*, 8 Femtos to cover the entire floor #1 ($F = 8$ *i.e.*, $F1, F2, \ldots, F8$) as shown in Fig. 11 and 12 Femtos to cover the floor #2 ($F = 12$ *i.e.*, $F1, F2, \ldots, F12$) as shown in Fig. 12. Fig. 11 shows SNR heat map on the floor #1 along with Femtos locations. The darker region in SNR heat map represents the Femto locations with high SNR value with an indoor path loss constant of $\alpha = 3.5$. In Fig. 11, the Femto $F1$ and $F2$ are deployed very close to the wall. For users within the boundaries of the four walls in which the Femto is present, a good SNR in the range of 15 to 35 dB can be guaranteed. But, when the signal has to cross a wall to reach the user, the range of SNR guaranteed decreases drastically to -2 to 15 dB. This is because the signal attenuates faster and degrades the signal strength in the presence of walls. As the distance increases from the Femto, most of the sub-regions get only 0 to 5 dB. Similar trend can be observed on the floor #2, refer Fig. 12.

Fig. 13 shows the connectivity region of each of the Femtos on the floor #1. The same colored sub-regions are connected to the same Femto. The average number of sub-regions served by a Femto on floor #1 is more when compare to floor #2, which is due to the large deployment of Femtos in the latter. Similarly, the connectivity region of the floor #2 is shown in Fig. 14.
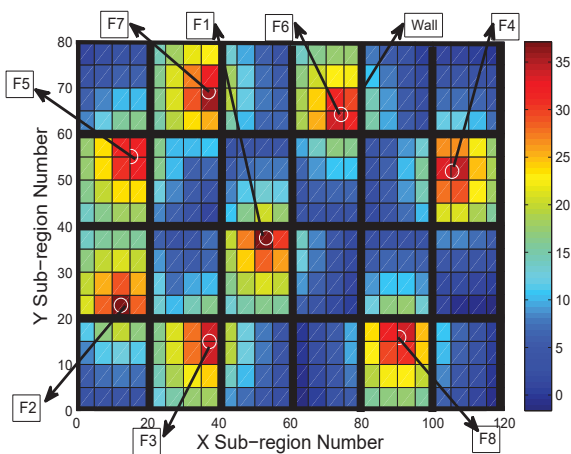
Figure 11. SNR distribution and Femto locations given by optimal Femto placement model for uniform UE distribution on the floor #1.
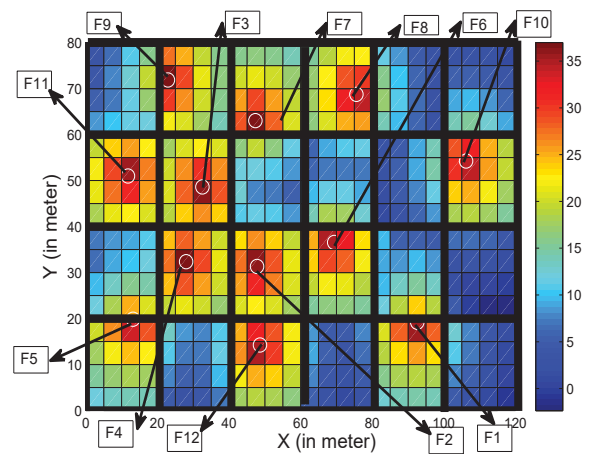

Figure 12. SNR distribution and Femto locations given by optimal Femto placement model for uniform UE distribution on the floor #2.
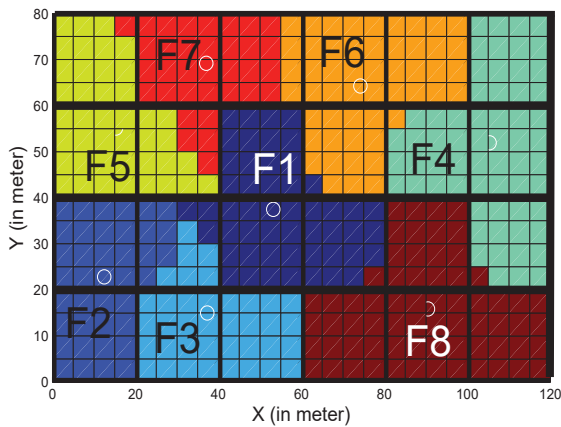

Figure 13. Femto Connectivity Region for uniform UE distribution on the floor #1.
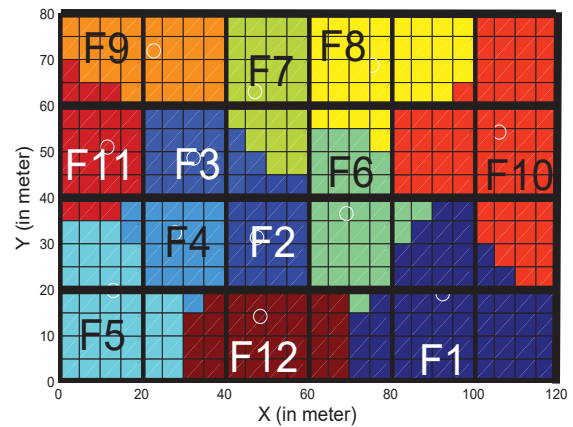

Figure 14. Femto Connectivity Region for uniform UE distribution on the floor #2.

B. Non-uniform UE Distribution

If the density of UEs is of non-uniform (e.g., random), the proposed Femto placement model still works and provides placement, however, it may lead to coverage holes inside the building. To demonstrate this, we took non-uniform distribution of UEs as shown in Fig. 15. Here we assumed that there are no UEs in the center region of a one-floor building (represented by blue color in Fig. 15). Based on this UE density, Fig. 16 shows the total number of Femtos required (i.e., F= 8) as per the proposed Femto placement model and their connectivity regions. Fig. 17 shows SNR distribution across sub-regions inside the building. The darker region in SNR heat map represents the Femto location with high SNR value. The SNR observed in the center

region of the building is < -5 dB and hence there is a coverage hole.

5.2. Performance of the Proposed System when the UE Traffic Demand is Uniform

In the following, we consider Femto deployment by assuming uniform UE distribution to avoid coverage holes inside the building and study the performance of the coupled and decoupled systems in the case of uniform UE traffic demand in the network.

A. Performance of the Proposed Offloading Algorithm

In order to analyze the performance of our proposed offloading algorithm we have considered the UE distribution as shown in Figs. 18 and 19. The placement
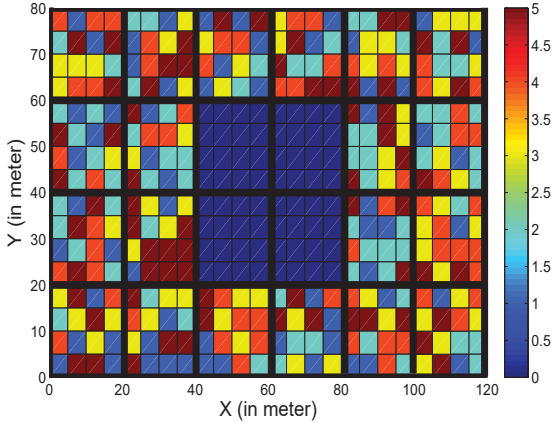
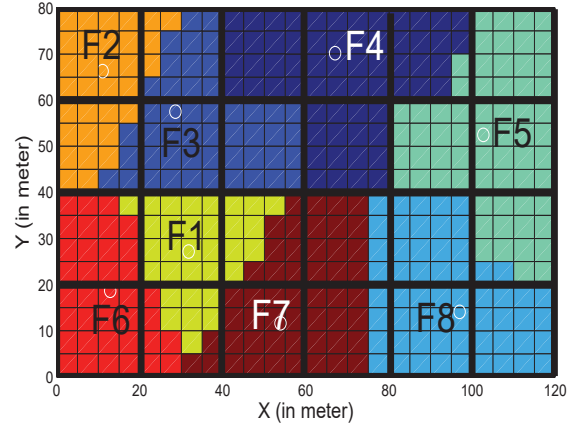**Figure 15.** A building's floor with non–uniform UE distribution.

Figure 16. Femto connectivity region for non–uniform UE distribution given in Fig. 15.
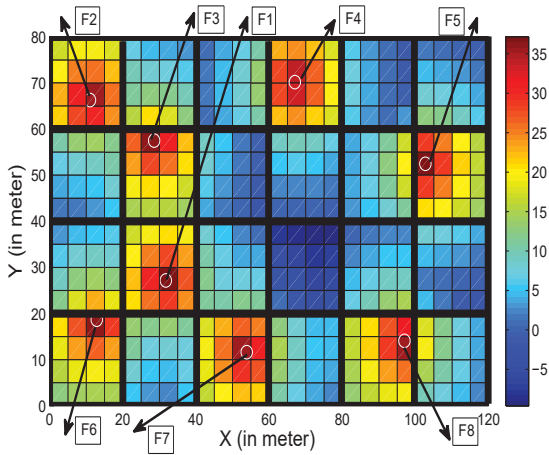

Figure 17. SNR distribution and Femto locations given by optimal Femto placement model for non–uniform UE distribution given in Fig. 15.

of Femtos which is based on a uniform distribution of UEs having same data demand implies that the load across all Femtos is uniform. The assumptions of a uniform UE distribution and an equivalent data demand cannot be employed to evaluate the efficiency of our proposed offloading algorithm. To show the potential of proposed offloading algorithm, we assumed non-uniform UE distribution with fixed traffic (i.e., 400 Kbps).

(a) UE Connectivity Before and After Offloading

Fig. 20 shows the user downlink connection before and after offloading on floor #1. The Femtos are represented as $\triangledown$, while the users are shown as $*$, $\star$, $\circ$, $\bullet$, $\square$, $\blacksquare$, $\diamond$, or $+$ having the respective boundary color of the corresponding *serving* Femto which is serving them. The red lines show the offloaded UEs

and their corresponding *target* Femtos after offloading. The Femtos $F1$, $F3$, $F4$, $F5$ and $F7$ are lightly loaded with lesser user count, but the other Femtos ($F2$, $F6$ and $F8$) are heavily loaded. In our work, the offloading algorithm will choose the efficient and closest downlink pair (u^*, f^*) by checking the load with all the users from the overlapping neighboring Femtos in such a way that the throughput and load are well balanced. The reason for the offloading algorithm to choose the shortest downlink attachment is due to efficient usage of RBs. Otherwise, it requires more bandwidth from the neighboring Femtos due to less SNR. For example, the Femto $F2$ is heavily loaded but the neighboring Femtos ($F3$ and $F5$) are lightly loaded. Our offloading algorithm offloads 5 UEs ($u1$, $u2$, $u3$, $u4$ and $u5$) to Femtos $F3$ and $F5$. Similarly $F1$ chooses the one cell edge UE ($u6$) from $F8$ for offloading by the neighboring Femtos. Hence, the total number of offloaded downlink user-Femto pair is represented as $U1$, $U2$, ..., $U7$ respectively.

Fig. 21 shows the downlink offloading on floor #2. Here, most of the Femtos ($F1$, $F7$, $F9$, $F10$, $F12$) are heavily loaded due to large number of UEs. Observations similar to the ones made in the floor #1 scenario can be made in this case as well.

(b) Required RBs in each Femto

Fig. 22 shows the required RBs for each Femto ($TotDemand_f$) on floor #1 before and after offloading. Before offloading, Femtos $F2$, $F6$ and $F8$ require excess number of RBs (i.e., 3400000 RBS which is greater than the limit[1], 2500000 RBs) due to heavy load and receive less SNR values because of walls. Femto $F2$

---

[1]The limits depends on spectrum bandwidth allotted for each BS by the network operator. In our scenario the total amount of bandwidth is 5 MHz (i.e., 25 RB). Simulation is done for 100 s. Hence, the total available RBs is 2500000 RB.
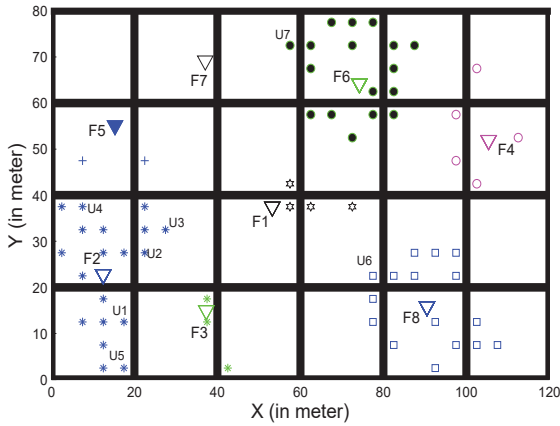
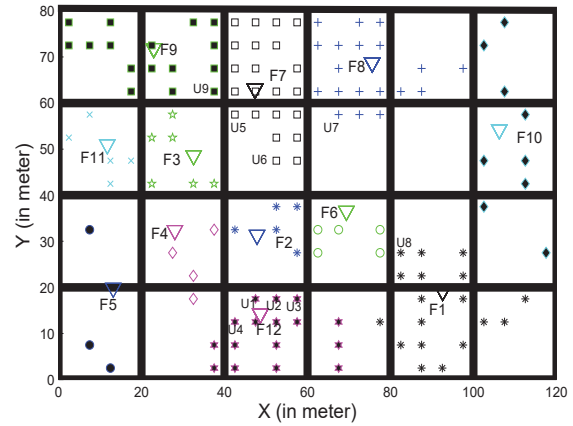**Figure 18.** UE Distribution on floor #1 for uniform traffic pattern.

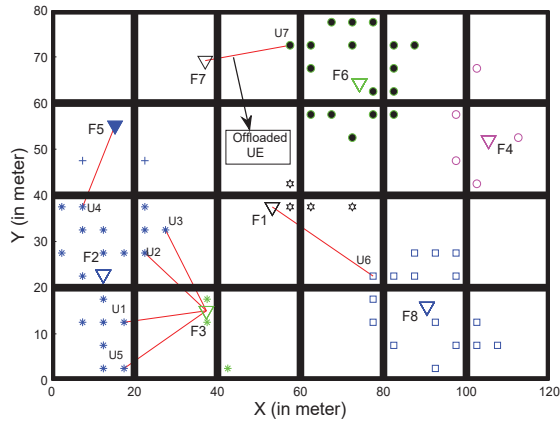**Figure 19.** UE Distribution on floor #2 for uniform traffic pattern.

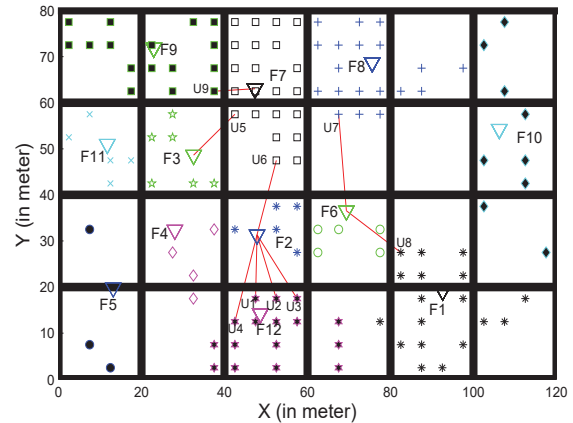**Figure 20.** UE Connectivity before and after Offloading on floor #1 for uniform traffic pattern.

Figure 21. UE Connectivity before and after Offloading on floor #2 for uniform traffic pattern.

has two overlapping *target* Femtos (i.e., $F3$ and $F5$) as shown in Fig. 20. But, the Femtos $F3$ and $F5$ are lightly loaded and require only 400000 RBs and 200000 RBs respectively, which is lesser than the limit, 2500000 RBs. So, the *target* Femtos can share the RBs with the heavily loaded *serving* Femto $F2$ which brings down $F2$'s requirement to 2200000 RBs. Similarly, $F6$ also needs excess RBs due to heavy load (refer Fig. 20). The overlapping Femto $F7$ can balance the load by sharing their RBs. Hence, minimum data rate (i.e., 400 Kbps) is maintained for all users in each Femto. Further, to guarantee more than the minimum data rate and to ensure fairness among all UEs. Operator should incorporate existing scheduling algorithm like proportional fair during offloading (But it is beyond the scope of our work). Similar pattern can be observed on floor #2 for Femtos $F12$, $F7$ and $F8$ (Fig. 23).

(c) Downlink User Count

Fig. 24 shows the user count on floor #1 for each Femto before and after offloading. If we observe Fig. 24, the number of users in Femto $F2$ is very high before offloading. After offloading with *target* Femtos $F3$ and $F5$, five users have been offloaded. This reduces the load in the overloaded Femto $F2$ and the QoS demand for the remaining connected users in Femto $F2$ is guaranteed.

Similarly, Fig. 25 shows the user count on floor #2 for each Femto before and after offloading. The load in Femtos $F1$, $F7$, $F9$, $F10$ and $F12$ was high due to higher number of users. Since $F2$ is closer, more number of users from $F12$ got offloaded to $F2$.

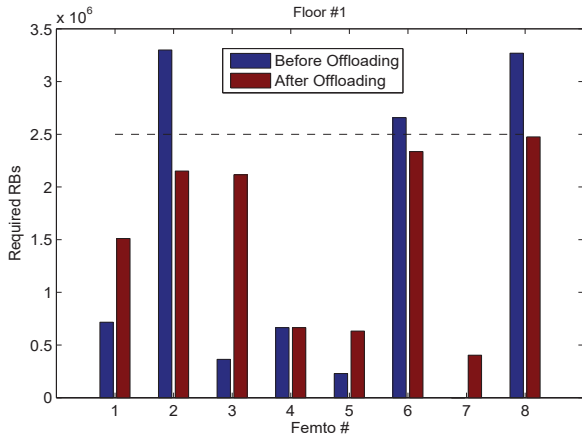## B. Comparison between Coupled and Decoupled Access Systems

Figure 22. $TotDemand_f$ of each Femto before and after offloading on floor #1 for uniform traffic pattern.
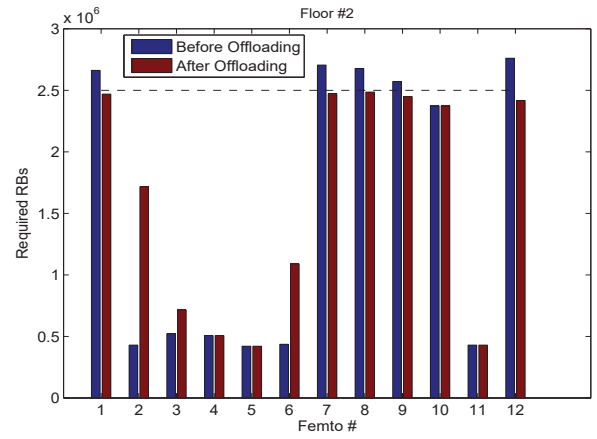

Figure 23. $TotDemand_f$ of each Femto before and after offloading on floor #2 for uniform traffic pattern.
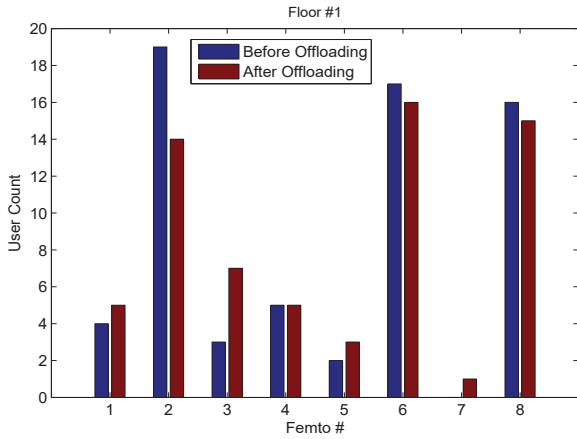

Figure 24. Downlink user count in each Femto before and after offloading on floor #1 for uniform traffic pattern.
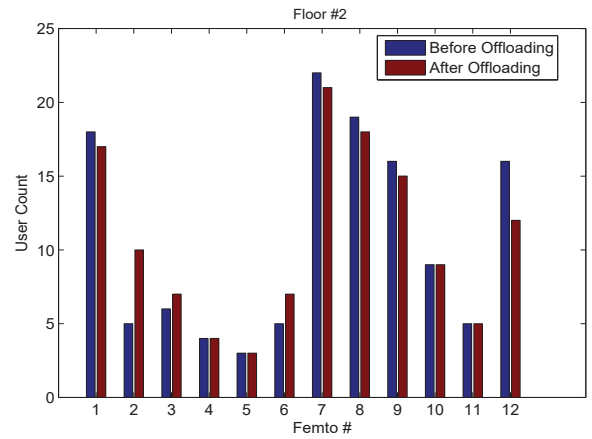

Figure 25. Downlink user count in each Femto before and after offloading on floor #2 for uniform traffic pattern.

We show the SNR value of the offloaded UEs when they transmit with full power in *coupled* and *decoupled* access systems. For the fixed uplink SNR, we also show the advantages in terms of the transmission power when UEs are in *coupled* and *decoupled* access systems.

(a) Maximum Achieved Uplink SNR

Fig. 26 shows the maximum SNR value that the UEs can achieve in full power transmission when it connect to the *serving* Femto or the *target* Femto on floor #1. Due to heavy load in $F8$, the user ($u6$) got offloaded to $F1$. The user $u6$ receives roughly +1 dB SNR during uplink from *serving* Femto $F8$ because it has to cross 2 walls. Thus for the same uplink transmission power, when it gets connected to the *target* Femto, it receives very less i.e., roughly -1 dB SNR because it is located in the cell edge of Femto $F1$.

Fig. 27 shows the maximum SNR value achieved on floor #2. As the Femtos are densely deployed on floor #2, the inter distance between the Femtos is very less (refer Fig. 21). This assists most of the users to achieve better SNR value when compared to floor #1. Even after offloading 9 users, all of them are able to achieve a decent SNR value. Compared to *decoupled* access system in floor #1 and floor #2, uplink SNR has decreased by 52% in *coupled* access system.

(b) Uplink Power to maintain $SNR = 0\ dB$

Fig. 28 shows the uplink power emitted by the downlink offloaded UEs to maintain $SNR = 0$ dB for floor #1. In this scenario, the *serving* Femto will always allow the UE to transmit with less power due to shorter distance. For example, to maintain $SNR = 0$ dB, the UE $u6$ transmits 0.09 W to the *serving* Femto. If the same UE wants to connect with the *target* Femto, it
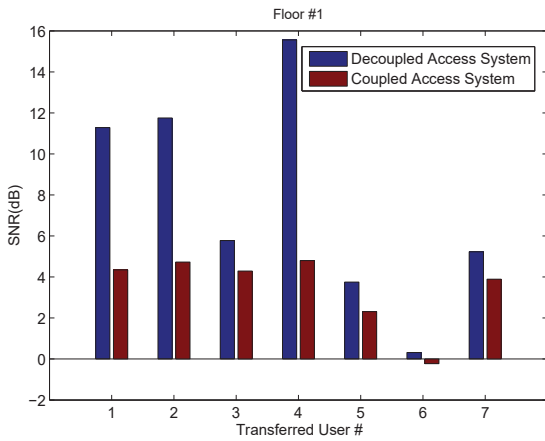
Figure 26. Maximum Achieved Uplink SNR in *coupled* and *decoupled* access systems on floor #1 for uniform traffic pattern.
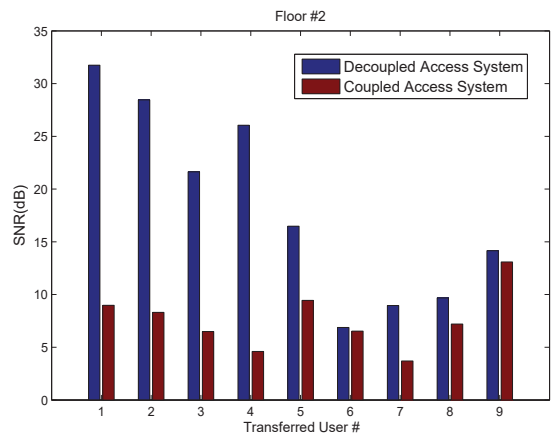

Figure 27. Maximum Achieved Uplink SNR in *coupled* and *decoupled* access systems on floor #2 for uniform traffic pattern.
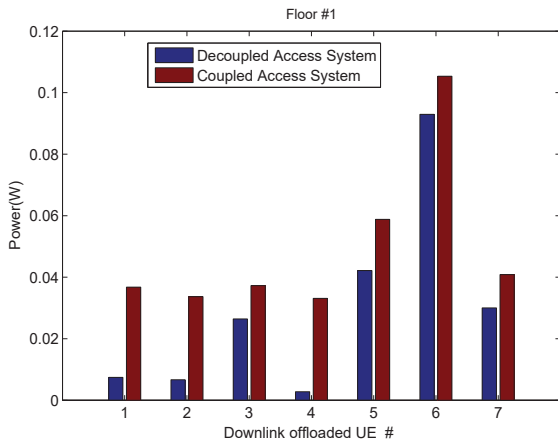

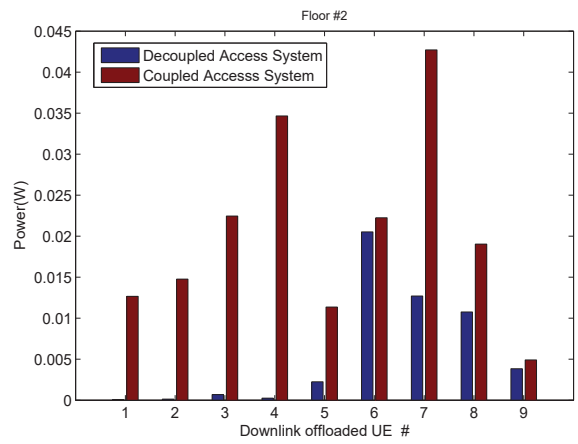**Figure 28.** Power emitted by UE in *coupled* and *decoupled* access systems on floor #1 for uniform traffic pattern.

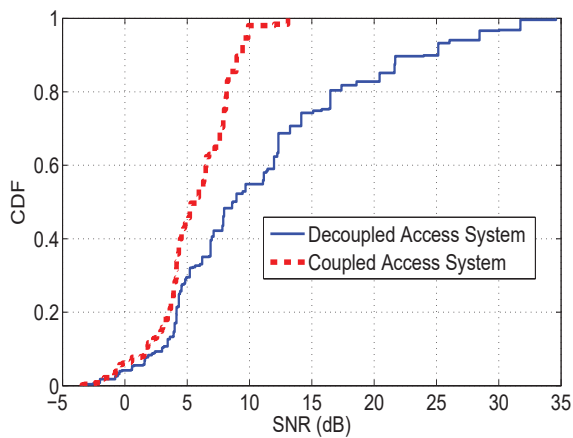**Figure 29.** Power emitted by UE in *coupled* and *decoupled* access systems on floor #2 for uniform traffic pattern.

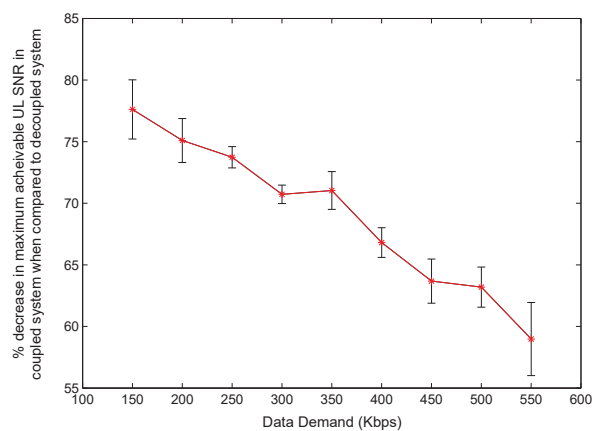**Figure 30.** CDF of the maximum Achieved Uplink SNR in *coupled* and *decoupled access systems.*

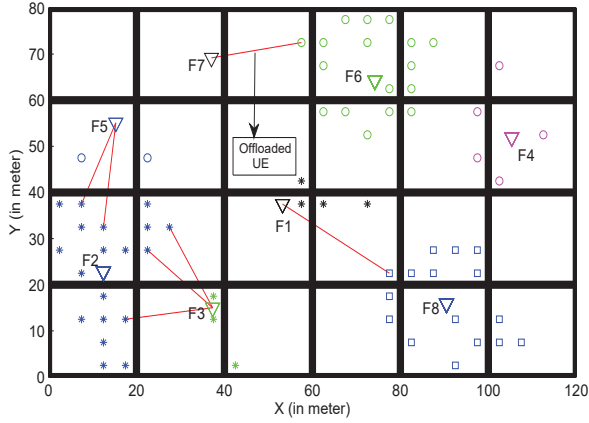**Figure 31.** Confidence Interval for Different Data Demand

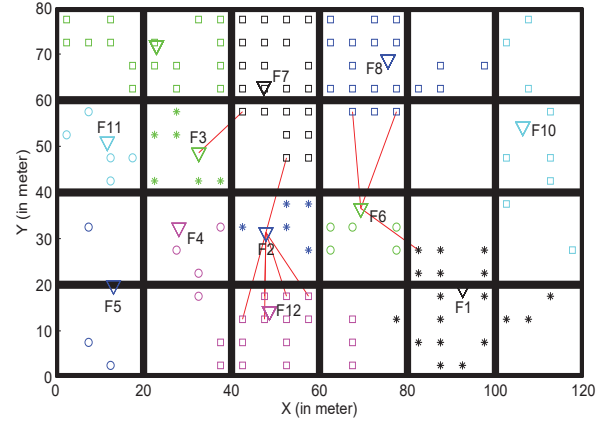**Figure 32.** UE Connectivity before and after Offloading on floor #1 for non-uniform traffic pattern.

Figure 33. UE Connectivity before and after Offloading on floor #2 for non-uniform traffic pattern.
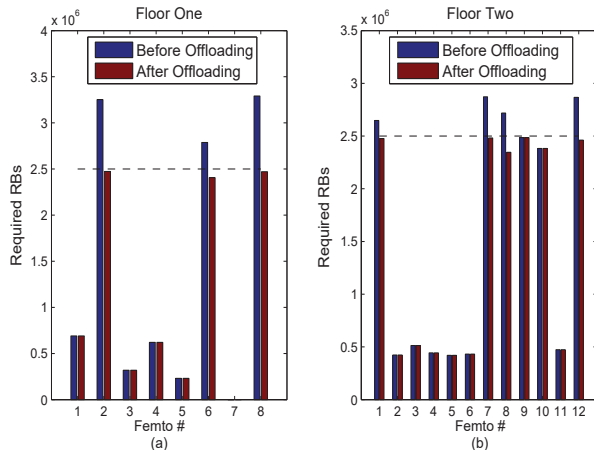

Figure 34. $TotDemand_f$ of each Femto before and after offloading on floor #1 and floor #2 for non-uniform traffic pattern.
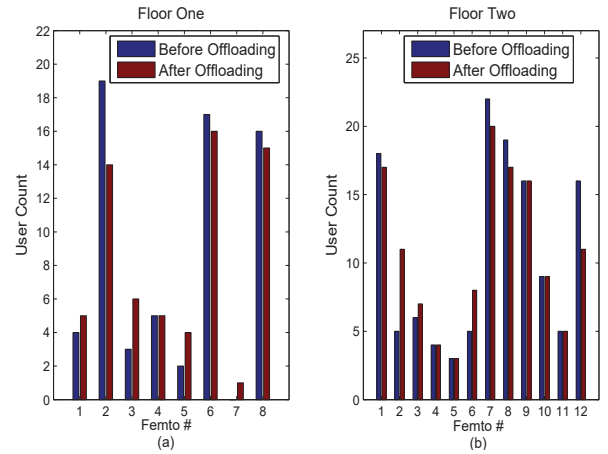

Figure 35. User count in each Femto before and after offloading on floor #1 and floor #2 for non-uniform traffic pattern.

has to transmit > 0.1 W. However, according to 3GPP standard, the user cannot maintain communication with the *target* Femto. To maintain communication with the *target* Femto, the user has to tune its SNR threshold to less than 0 dB.
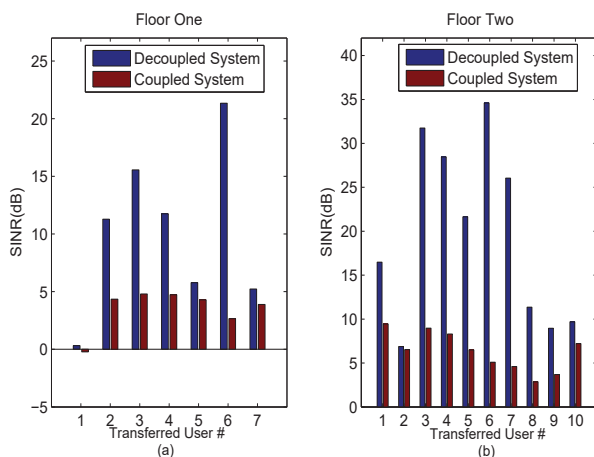
Fig. 29 shows the uplink power emitted by the downlink offloaded UEs to maintain $SNR = 0$ dB for floor #2. Due to dense deployment of Femtos and less inter distance between them, the uplink power is reduced drastically when compare to floor #1. For example most of the UEs among the 9 are allowed to transmit with less power (i.e., 0.025 W) in closer Femto. As the UE battery power plays an important role in wireless communication, we allow the UEs to communicate the uplink information to the closer Femto. Thus the decouple system helps in saving power. Compared to *coupled* access system in floor #1 and floor #2, uplink power has reduced by 56% in

decoupled access system.

C. Average Performance of the Proposed System

We performed the simulation for 30 different scenarios (i.e., UE distribution is varied arbitrarily by changing the seed value) with the fixed traffic pattern (i.e., 400 Kbps) and the following are the results.

Fig. 30 shows the CDF of the maximum uplink SNR achieved in full power transmission by the transferred UEs in the *decoupled access system* and the *coupled access system*. On an average, compared to *decoupled access system*, maximum achievable uplink SNR has decreased by 64% in *coupled access system*. For a fixed uplink SNR threshold (i.e., 0 dB), on an average, the UE transmission power has reduced by 70% in *decoupled*

EAI
European Alliance
for Innovation

15

EAI Endorsed Transactions on
Future Internet
03 – 05 2016 | Volume 3 | Issue 9 | e2

Figure 36. Maximum Achieved Uplink SNR in *coupled* and *decoupled* access systems on floor #1 and floor #2 for non-uniform traffic pattern.
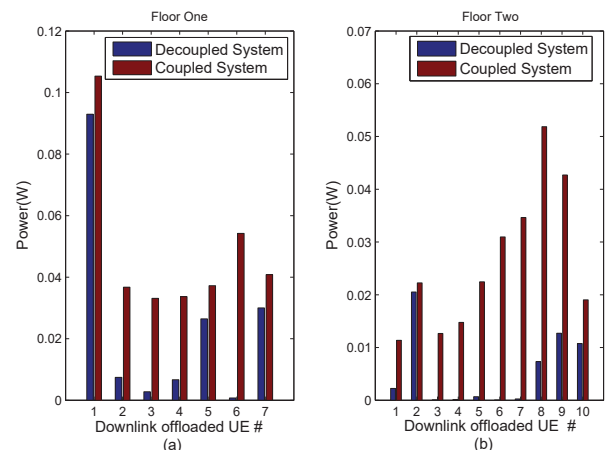
Figure 37. Power emitted by UE in *coupled* and *decoupled* access systems on floor #1 and floor #2 for non-uniform traffic pattern.

access system when compared to the *coupled access system*.

We then vary traffic from 150 Kbps to 550 Kbps in the steps of 50 Kbps in 9 experiments in such a way that all UEs in any given experiment generate fixed traffic in the above interval of (150 Kbps to 550 Kbps). Each experiment was ran for 30 seeds. In Figure 31, X-axis shows the variation in traffic demand and Y-axis shows the percentage decrease in achievable uplink SNR in *coupled access system* when compared to the proposed *decoupled access system*. It is plotted with 95% confidence intervals..

5.3. Performance of the Proposed System when the UE Traffic Demand is non–uniform

In the following, we consider Femto deployment given by uniform UE distribution and study the performance of the proposed system in the case of non-uniform UE traffic demand (i.e., 300 to 500 Kbps).

As explained in fixed traffic pattern (Section 5.2), the same optimal placement model is used with the assumption of uniform UE distribution. The UE distribution on floor #1 and #2 is same as shown in Figs. 18 and 19. We assumed that the traffic patterns are varied from 300 Kbps to 500 Kbps in the steps of 10 Kbps. That means UEs arbitrarily select some traffic pattern in the interval of (300 Kbps to 500 Kbps). Fig. 32 shows the user downlink connection before and after offloading on floor #1. Similarly Fig. 33 shows the user downlink connection before and after offloading on floor #2. Note that all the observations are as similar to what had been reported for the uniform UE distribution and only the offloading UEs will differ

based on the traffic load (i.e.. traffic pattern).

Fig. 34 (a) and Fig. 34 (b) show the required RBs for each Femto ($TotDemand_f$) on floor #1 and floor #2 before and after offloading. Fig. 35 (a) and Fig. 35 (b) show the user count on floor #1 and floor #2 for each Femto before and after offloading. We show the SNR value of the offloaded UEs when they transmit with full power in *coupled* and *decoupled* access systems. For the fixed uplink SNR, we also show the advantages in terms of the transmission power when UEs are in *coupled* and *decoupled* access systems. Fig. 36 (a) and Fig. 36 (b) show the maximum SNR value that the UEs can achieve in full power transmission when it connect to the *serving* Femto or the *target* Femto on floor #1 and floor #2. Similarly, Fig. 37 (a) and Fig. 37 (b) show the uplink power emitted by the downlink offloaded UEs to maintain $SNR = 0$ dB for floor #1 and floor #2.

6. Conclusions and Future work

In this paper, considering realistic constraints, we have provided an MILP model for the optimal placement of Femtos based on user occupant probabilities inside an enterprise building scenario to achieve desirable signal strengths for all the users. We conducted extensive experiments in MATLAB to demonstrate the benefits of proposed optimal placement model. We established DuD connections based on the shortest-path loss Femto for the uplink access and a less loaded neighboring Femtos for the downlink access. On average we observed 70% energy savings in *decoupled* access system when compared to the traditional *coupled* access system. In future, we intend to consider more complex scenarios involving cross-tier and co-tier interference in the system model and guarantee SINR even at the farthest point in the sub-regions. Also would like to employ

different access modes of Femtos while providing an algorithm for optimal Femto placement.

References

[1] "Views on rel-12 and onwards for lte and umts." Future Radio in 3GPP, Huawei Technologies, 2012.

[2] V. Chandrasekhar, J. Andrews, and A. Gatherer, "Femtocell networks: a survey," *Communications Magazine, IEEE*, vol. 46, no. 9, pp. 59–67, 2008.

[3] "3gpp femtocells: Architecture and protocols." Qualcomm Inc., Sept. 2010.

[4] Z. Shen, A. Khoryaev, E. Eriksson, and X. Pan, "Dynamic uplink-downlink configuration and interference management in td-lte," *Communications Magazine, IEEE*, vol. 50, no. 11, pp. 51–59, 2012.

[5] T. Nakamura, S. Nagata, A. Benjebbour, Y. Kishiyama, T. Hai, S. Xiaodong, Y. Ning, and L. Nan, "Trends in small cell enhancements in lte advanced," *Communications Magazine, IEEE*, vol. 51, no. 2, pp. 98–105, 2013.

[6] H. Wang, L. Ding, P. Wu, Z. Pan, N. Liu, and X. You, "Dynamic load balancing in 3gpp lte multi-cell networks with heterogenous services," in *Communications and Networking in China (CHINACOM), 2010 5th International ICST Conference on*, pp. 1–5, IEEE, 2010.

[7] H. Wang, L. Ding, P. Wu, Z. Pan, N. Liu, and X. You, "Qos-aware load balancing in 3gpp long term evolution multi-cell networks," in *Communications (ICC), 2011 IEEE International Conference on*, pp. 1–5, IEEE, 2011.

[8] "GAMS." http://www.gams.com/.

[9] W. Guo, S. Wang, X. Chu, J. Zhang, J. Chen, and H. Song, "Automated small-cell deployment for heterogeneous cellular networks," *Communications Magazine, IEEE*, vol. 51, no. 5, pp. 46–53, 2013.

[10] W. Guo and S. Wang, "Interference-aware self-deploying femto-cell," *Wireless Communications Letters, IEEE*, vol. 1, no. 6, pp. 609–612, 2012.

[11] R. Liu, I. J. Wassell, and K. Soga, "Relay node placement for wireless sensor networks deployed in tunnels," in *IEEE WiMob, 2010 IEEE 6th International Conference on*, pp. 144–150, IEEE, 2010.

[12] S. S. Dhillon, K. Chakrabarty, and S. Iyengar, "Sensor placement for grid coverage under imprecise detections," in *Information Fusion, 2002. Proceedings of the Fifth International Conference on*, vol. 2, pp. 1581–1587, IEEE, 2002.

[13] A. Capone, M. Cesana, D. De Donno, and I. Filippini, "Optimal placement of multiple interconnected gateways in heterogeneous wireless sensor networks," in *NETWORKING 2009*, pp. 442–455, Springer, 2009.

[14] J. Zhang, X. Jia, Z. Zheng, and Y. Zhou, "Minimizing cost of placement of multi-radio and multi-power-level access points with rate adaptation in indoor environment," *Wireless Communications, IEEE Transactions on*, vol. 10, no. 7, pp. 2186–2195, 2011.

[15] V. Sathya, A. Ramamurthy, and B. R. Tamma, "On placement and dynamic power control of femtocells

[16] V. Sathya, A. Ramamurthy, and B. Tamma, "Joint placement and power control of lte femto base stations in enterprise environments," in *Computing, Networking and Communications (ICNC), 2015 International Conference on*, pp. 1029–1033, Feb 2015.

[17] J. Liu, T. Kou, Q. Chen, and H. D. Sherali, "Femtocell base station deployment in commercial buildings: A global optimization approach," *Selected Areas in Communications, IEEE Journal on*, vol. 30, no. 3, pp. 652–663, 2012.

[18] J. Liu, Q. Chen, and H. D. Sherali, "Algorithm design for femtocell base station placement in commercial building environments," in *INFOCOM, 2012 Proceedings IEEE*, pp. 2951–2955, IEEE, 2012.

[19] Z. Li, H. Wang, Z. Pan, N. Liu, and X. You, "Joint optimization on load balancing and network load in 3gpp lte multi-cell networks," in *Wireless Communications and Signal Processing (WCSP), 2011 International Conference on*, pp. 1–5, IEEE, 2011.

[20] R. Chaganti, V. Sathya, S. A. Ahammed, R. Rex, and B. R. Tamma, "Efficient son handover scheme for enterprise femtocell networks," in *Advanced Networks and Telecommuncations Systems (ANTS), 2013 IEEE International Conference on*, pp. 1–6, IEEE, 2013.

[21] H. Elshaer, F. Boccardi, M. Dohler, and R. Irmer, "Downlink and uplink decoupling: a disruptive architectural design for 5g networks," *arXiv preprint arXiv:1405.1853*, 2014.

[22] K. Smiljkovikj, P. Popovski, and L. Gavrilovska, "Analysis of the decoupled access for downlink and uplink in wireless heterogeneous networks," *Wireless Communications Letters, IEEE*, vol. 4, no. 2, pp. 173–176, 2015.

[23] M. Tahalani, V. Sathya, A. Ramamurthy, U. Suhas, M. K. Giluka, and B. R. Tamma, "Optimal placement of femto base stations in enterprise femtocell networks," in *Advanced Networks and Telecommuncations Systems (ANTS), 2014 IEEE International Conference on*, pp. 1–6, IEEE, 2014.

[24] D.-h. Sung, J. S. Baras, and C. Zhu, "Coordinated scheduling and power control for downlink cross-tier interference mitigation in heterogeneous cellular networks," in *Global Communications Conference (GLOBECOM), 2013 IEEE*, pp. 3809–3813, IEEE, 2013.

[25] N. Saquib, E. Hossain, L. B. Le, and D. I. Kim, "Interference management in ofdma femtocell networks: Issues and approaches," *Wireless Communications, IEEE*, vol. 19, no. 3, pp. 86–95, 2012.

[26] M. T. Kawser, N. I. B. Hamid, M. N. Hasan, M. S. Alam, and M. M. Rahman, "Downlink snr to cqi mapping for different multiple antenna techniques in lte,"

[27] F. Boccardi, J. Andrews, H. Elshaer, M. Dohler, S. Parkvall, P. Popovski, and S. Singh, "Why to decouple the uplink and downlink in cellular networks and how to do it," *arXiv preprint arXiv:1503.06746*, 2015.

in lte hetnets," in *Global Communications Conference (GLOBECOM), 2014 IEEE*, pp. 4394–4399, Dec 2014.